Water Research 281 (2025) 123576

Contents lists available at ScienceDirect

Water Research

journal homepage: www.elsevier.com/locate/watres

Intensifying methane emissions in Chinese Ponds: The interplay of warming, eutrophication, and depth changes

Mingquan Lv, Ping Huang, Xin Gao, Jilong Chen, Shengjun Wu *

Chongqing Institute of Green and Intelligent Technology, Chinese Academy of Sciences, Chongqing 401122, China

ARTICLE INFO

Keywords:
Methane ebullition
Nutrient enrichment
Spatially explicit
Temperature dependence
Small waterbodies

ABSTRACT

Ponds are significant contributors to global methane (CH_4) emissions. However, accurately estimating their historical or future CH_4 emissions remains challenging, particularly under dynamic environmental changes such as eutrophication, sedimentation-driven shallowing, and global warming. We synthesized 674 observations of CH_4 emission rates to identify key drivers and develop a process-based predictive model. We present a framework for spatially explicit estimation of pond CH_4 emissions in China from 1960 to 2020, accounting for factors such as temperature dependence, depth, nutrient levels, and pond area. Our findings show that pond CH_4 emissions are strongly temperature-dependent, characterized by a high average activation energy (0.834 eV). Notably, ebullitive emissions exhibit greater temperature sensitivity than diffusive emissions. Nitrogen concentrations and water column depth emerged as critical predictors of total CH_4 fluxes. Over the past six decades, CH_4 emissions from Chinese ponds increased approximately 9-fold, from 0.16 Tg CH_4 yr^{-1} in 1960 to 1.53 Tg CH_4 yr^{-1} by 2020, emphasizing their growing role in global methane emissions. Notably, half of these emissions occur during summer, with ebullition accounting for 66 % of the total CH_4 flux. This increase was primarily driven by the interactions of warming, nutrient enrichment, declining water depth, and pond expansion. Our results underscore the growing role of ponds in CH_4 emissions and highlight the urgent need for mitigation measures, such as reducing nutrient loading and implementing periodic dredging management. This study provides a robust foundation for improving CH_4 emission estimates and developing sustainable management practices for ponds in the context of global environmental change.

1. Introduction

The atmospheric concentration of methane (CH_4) has nearly tripled from its estimated pre-industrial equilibrium value, making it the second most significant greenhouse gas (Kirschke et al., 2013; Saunois et al., 2020). Freshwater ecosystems contribute nearly half of the global CH_4 emissions to the atmosphere (Rosentreter et al., 2021). Historically, ponds have been overlooked in studies of regional and global aquatic carbon cycles, and the focus has been on estimating carbon fluxes from larger water bodies, such as lakes and reservoirs (Deemer et al., 2016; Ran et al., 2021; Raymond et al., 2013). Despite small size, ponds collectively cover an estimated global surface area of over 0.55 million km^2 defined as smaller than 1 ha and >1.23 million km^2 when considering those under 10 ha (Holgerson and Raymond, 2016). As a key part of aquatic ecosystems globally, ponds are notable sources of CH_4 emissions due to their shallow depth and high nutrient inputs (Holgerson and Raymond, 2016). However, significant challenges remain in accurately estimating historical or even predicting future CH_4 emissions from ponds.

Most pond CH_4 measurements have been collected in boreal regions (Bastviken et al., 2011; Holgerson and Raymond, 2016; Wik et al., 2016), where ponds tend to be less productive and experience lower human disturbance. Recently, studies on CH_4 emissions from ponds in tropical and temperate regions—often characterized by higher human impact and eutrophication—have been increasing (Malerba et al., 2022b; Ray et al., 2023; van Bergen et al., 2019; Zhao et al., 2025). Ebullition is typically the dominant pathway for total CH_4 flux, contributing 50 % to over 90 % of emissions (Bastviken et al., 2004). However, many past studies have overlooked ebullition when quantifying CH_4 emissions from ponds (Ollivier et al., 2019; Peacock et al., 2019; Webb et al., 2019). More recent work has begun addressing this gap by incorporating ebullitive flux measurements (Naslund et al., 2024; Yang et al., 2020). Together, these studies provide a basis for understanding drivers of CH_4 fluxes from ponds over a wide geographic scale.

* Corresponding author.
E-mail address: wsj@cigit.ac.cn (S. Wu).

https://doi.org/10.1016/j.watres.2025.123576
Received 3 January 2025; Received in revised form 28 March 2025; Accepted 29 March 2025
Available online 31 March 2025

Accurately estimating pond CH_4 flux is challenging and requires a mechanistic understanding of what regulates CH_4 emissions. Simplistic upscaling approach, based on average rates and surface area, can overestimate CH_4 flux by 70–100 % (Lauerwald et al., 2023a). Ponds are frequently grouped with lakes or reservoirs for CH_4 emission upscaling (DelSontro et al., 2018; Li et al., 2020). Ponds likely represents fundamentally distinct methane sources compared large water bodies due to their smaller size, shallower depth, and stronger hydrological connectivity with surrounding landscapes. These distinct characteristics position ponds as ideal model systems for studying aquatic ecosystem responses to global change. Ponds receive a large amount of sediments and terrestrial-derived organic carbon due to their high lateral hydrological connectivity with surrounding landscapes (Downing et al., 2008). Smaller ponds, in particular, undergo severe sedimentation (Lv et al., 2024). These high sedimentation rates supply reactive organic matter, driving CH_4 emissions through ebullition (Maeck et al., 2013; Sobek et al., 2012). Additionally, sediment-water column interface in ponds is highly sensitive to atmospheric temperature fluctuations due to shallow depth (Toffolon et al., 2014). This sensitivity accelerates the mineralization and decomposition of organic matter, leading to CH_4 production (Yvon-Durocher et al., 2014a). Correspondingly, ponds are likely to exhibit a stronger temperature dependence for CH_4 emissions compared to larger water bodies (DelSontro et al., 2016; West et al., 2016). Unlike large lakes, ponds are often constructed for irrigation and other human uses, making them more susceptible to anthropogenic influence. Those located near agricultural lands are particularly vulnerable to eutrophication due to high nutrient inputs from agricultural non-point sources (Goyal et al., 2021; Meng et al., 2022). Eutrophication further amplifies CH_4 emissions (Beaulieu et al., 2019). Therefore, understanding how CH_4 emissions are affected by these physical, chemical, and biological factors will be key in predicting pond CH_4 fluxes.

China serves as a large-scale “laboratory” for exploring how environmental changes, human activities, and pond expansion influence CH_4 emissions from ponds at the national scale. China has constructed a large number of ponds for irrigation prior to 1970s and now hosts 14.6 million ponds (defined as water bodies <5 ha in size) (Lv et al., 2022). The estimated cumulative water area of China’s ponds is equivalent to 42 % of total lake (Tao et al., 2020) and 68 % of reservoir area (Song et al., 2022), highlighting their significance as landscape features. Chinese intensive agricultural practices, which consume about 30 % of global fertilizer, generate substantial non-point source pollution (Gu et al., 2015). Due to close proximity to croplands and high hydrological connectivity to surrounding landscapes, ponds receive significant nutrient inputs from surface runoff, leading to increased primary productivity and exacerbated eutrophication (Lv et al., 2024; Xiao et al., 2024). These factors likely contribute to disproportionately high CH_4 emissions from ponds, underscoring the need to include them in national greenhouse gas inventories. However, no studies to date have quantified long-term CH_4 emissions from ponds, leaving a critical gap in understanding their contribution to greenhouse gas dynamics.

In this study, we compiled a global database of in situ CH_4 measurements (total, diffusive, and ebullitive fluxes) and relevant environmental variables, updated to 2024. We assessed the temperature sensitivity of different CH_4 emission pathways and identified potential drivers of CH_4 flux. Based on these primary drivers, we developed an optimized prediction model to upscale pond CH_4 emissions in China from 1960 to 2020, incorporating factors such as pond expansion, seasonal temperature variations, sedimentation and trophic state.

2. Methods

2.1. Data sampling and collection

Total CH_4 emission rates (diffusive and ebullitive emissions) were measured using the floating chamber technique (Natchimuthu et al., 2014) (Supplementary material S1) at ten ponds. The geographical location and key characteristics of these ponds are summarized in Table S1. The selection of these ponds was based on ensuring a diverse range of pond characteristics, particularly in terms of area, depth and cropland proportion, to capture different environmental conditions that influencing CH_4 emissions. Gas sampling was conducted at ten ponds across five seasons: summer (June, August), autumn (October), winter (December) in 2022, and spring (April) in 2023. Each sampling pond was equipped with three independent chambers for flux measurements. In-situ physical and chemical indicators such as water depth, water temperature, dissolved oxygen (DO), and Chlorophyll a (Chl-a) were measured by a YSI 6000 Multiprobe field meter. Additionally, three water samples were collected at a depth of 30 cm in each pond to analyze phosphorus and nitrogen and dissolved carbon concentrations, following the China National Standard Method (http://www.sac.gov.cn/).

We also conducted a comprehensive review of peer-reviewed literature on CH_4 emissions from ponds, published up to September 2024. Relevant publications were identified using keywords related to CH_4 emissions (‘CH_4 flux’, ‘CH_4 concentration’, ‘CH_4 emission’) and specific types of water bodies (‘stormwater pond’, ‘agricultural impoundment’, ‘pond’, ‘farm pond’, ‘agricultural pond’) across multiple academic databases, including Web of Science, and the China Knowledge Resource Integrated database (https://www.cnki.net). Overall, we gathered data on 624 CH_4 daily fluxes from different sites across 40 published papers and dissertations. Additional information collected included geographical coordinates (latitude and longitude), measurement timing, climatic factors (mean air temperature, mean precipitation, and water temperature), morphometric characteristics (e.g., surface area and water depth), trophic state indicator (Chl-a), dissolved organic carbon (DOC) and nutrient concentrations (nitrogen and phosphorus) for each of ponds.

Data were extracted from tables, figures, and texts within the identified publications, and digitized using Engauge Digitizer (version 11.0) when necessary. For observations lacking climate data, we obtained corresponding climate data from the WorldClim database (http://www.worldclim.org/), using site-specific latitude, longitude, and measurement timing. For cases where water temperature data were unavailable, we estimated values using a published relationship between air temperature (T_a) and water temperature (T), specifically: $T = 2.82 + 0.82T_a$ (Bai, 1999).

In total, we compiled 674 observations of CH_4 fluxes and associated environmental variables from both literature and in-field measurements (Table S2).

2.2. Temperature dependencies for CH_4 emissions

To estimate the temperature dependencies of pond CH_4 fluxes, we fitted the complied data using the Boltzmann–Arrhenius function (Yvon-Durocher et al., 2014b) by a linear mixing effect model:

$$\ln R_i(T) = \left(E + \epsilon_E^i\right)\left(\frac{1}{kT_C} - \frac{1}{kT}\right) + \ln R(T_C) + \epsilon_R^i \quad (1)$$

where $\ln R_i(T)$ represents the natural logarithm of the CH_4 flux rate at absolute temperature T (in Kelvin) for site *i; E* is the average apparent activation energy (eV) across sites, reflecting the temperature dependence of total (E_{TM}), diffusive (E_{DM})and ebulilitive (E_{EM}) CH_4 emissions; where k is the Boltzmann constant (8.62×10^{-5} eV k^{-1}). T_C (292 K, 19 °C) is the mean temperature of the dataset; therefore, so that $\ln R(T_C)$ represents the average CH_4 flux rate across sites at this reference temperature T_C. Site-specific variations in apparent activation energy and flux rates, due to biotic and abiotic factors, are captured by the terms ϵ_E^i and ϵ_R^i, which represent random deviations in the slopes and intercepts. We quantified the temperature dependence of the ebullition:total CH_4 emission ratio in exactly the same way as described above.

The linear mixed-effects modeling analysis was conducted using the 'lme' function in the 'nlme' package in *R* statistical software. Model fitting was assessed using likelihood ratio tests, with the optimal random effects structure identified by comparing Akaike Information Criterion (AIC) values for the null model (Perkins et al., 2012). To compare slopes derived from different datasets, Tukey's post hoc multiple comparison test was employed (Perkins et al., 2012).

2.3. Relationships between CH_4 emission rates against environmental factors

To explore the drivers of CH_4 emissions, daily CH_4 emission rates were standardized across sites and climates at 19 °C, using the fitted Boltzmann–Arrhenius relationship described in Section 2.2. Relationships between CH_4 emission rates and various environmental variables (e.g., climate factors, morphometric properties, nutrient levels, etc.) were examined using linear mixed-effects models. The models were generally specified as:

$$\ln R = \beta_0 + \beta_1 \times \ln X + \pi_{study} + \varepsilon \tag{2}$$

where, β_0 and β_1 are the intercept and slope, respectively; π_{study} is the random effect accounting for study-specific variation; ε is the sampling error; R and X correspond to the emission rate and environmental variable values, respectively, respectively. Random effects were included to account for potential biases between different studies.

2.4. Upscaling pond CH_4 from 1960 to 2020

To upscale CH_4 emissions from ponds across China, we first derived candidate models to predict total areal CH_4 flux at a standardized temperature of 19 °C, based on the compiled CH_4 emissions dataset. Potential predictor variables were selected from the results of Section 2.3. Multiple linear regression was applied to assess the influence of environmental variables on CH_4 emission fluxes, with both fluxes and predictor variables log-transformed to approximate normal distributions. The model with the high explanatory power (R^2) and better statistical significance was selected as the optimal model for upscaling.

Predicted CH_4 emission rates at the standard temperature were then adjusted to monthly emission rates (from January to December) based on temperature-dependent CH_4 emission patterns, following the equation:

$$\ln R_j(T) = \ln R(T_{19}) + E_{TM}\left(\frac{1}{kT_C} - \frac{1}{kT}\right) \tag{3}$$

where $R(T_{19})$ represents the predicted total areal CH_4 flux at a water temperature of 19 °C. $R_j(T)$ denotes the monthly actual CH_4 emission rate at water temperature T, $j = 1,2, \ldots, 12$. Monthly water temperatures for ponds were predicted based on the relationship between atmospheric and water temperatures (Bai, 1999), with monthly average atmospheric temperatures obtained from a 1-km monthly mean temperature dataset for China (1901–2022) (Peng, 2019).

Annual CH_4 fluxes were derived by summing monthly CH_4 fluxes across the year. Monthly CH_4 fluxes were calculated as the product of pond surface area, CH_4 emission rate, and the corresponding time period for each month. Upscaling analyses were conducted using hydrological level-8 (HL-8) river watersheds as the unit of calculation. The HydroATLAS database provided watershed delineations, dividing China into 13, 495 HL-8 watersheds (https://www.hydrosheds.org).

2.4.1. Pond area and depth

Ponds are generally defined by their small size and shallow depth. For this study, lentic waters with an area smaller than 5 hectares were

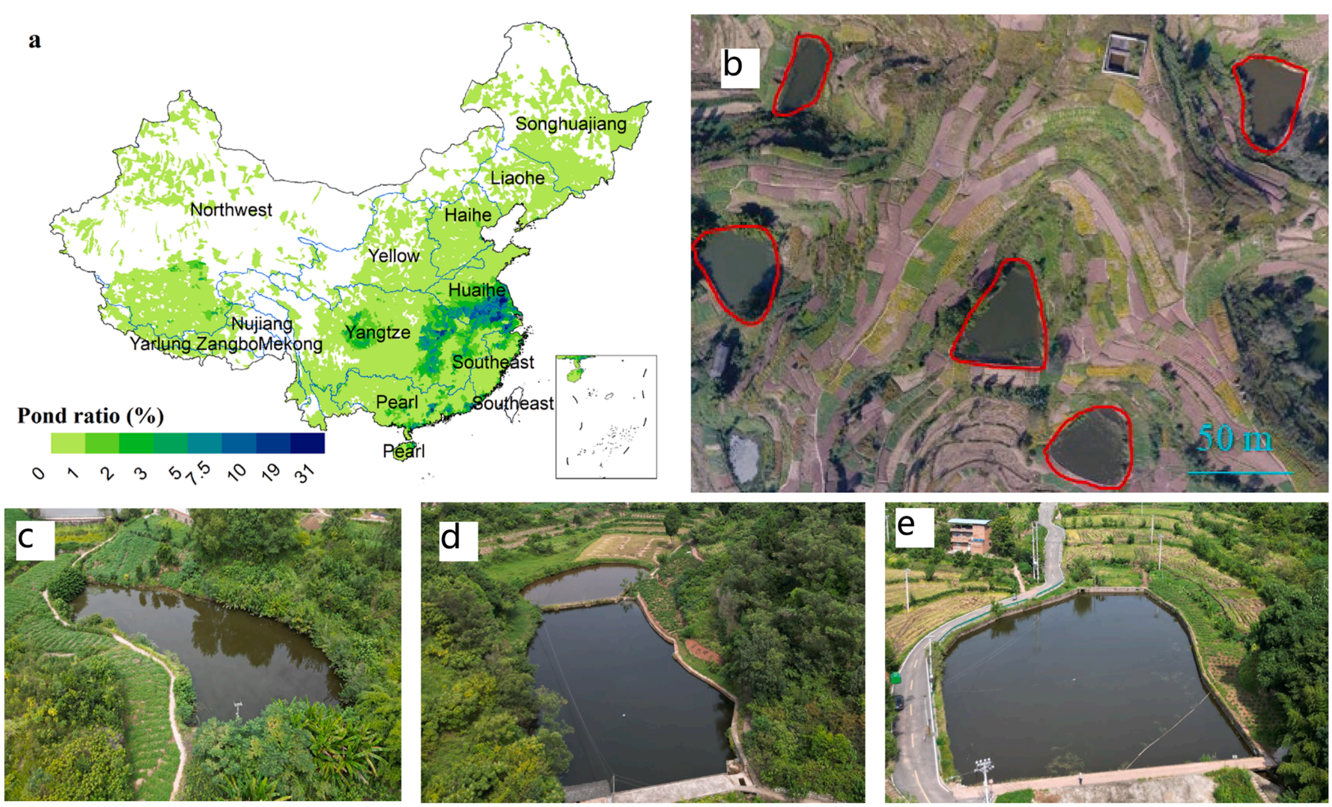

Fig. 1. Ponds in China. (a) Spatial distribution of ponds across China in 2018, adapted from Lv et al. (2022). (b) High-resolution imagery (Top-left: N31.222°, E108.357°; Bottom-right: N31.220°, E108.360°) showing close proximity of ponds to cultivated fields, acquired using an unmanned aerial vehicle platform. (c–e) Photographs of representative sampling ponds for CH_4 emissions: (c) Maliu (E106.607°, N29.947°), (d) Wangjia (E106.616°, N29.950°), and (e) Jintang (E106.624°, N29.955°).

classified as ponds (Richardson et al., 2022). According to this definition, China has approximately 14.6 million ponds covering a total area of 33,160 km^2 (Fig. 1a). Historical changes in the number and area of ponds from 1960 to 2020 were reconstructed using data from government bulletins published by China's Departments of Water Resources (Lv et al., 2024).

The depth of the pond has decreased due to sedimentation between 1960 and 2020. The original depth was calculated by dividing the pond's original storage capacity by its surface area. The original storage capacity was determined based on its relationship with surface area (Fig. S1). A previous study provided an approach to estimate sedimentation rates (cm yr^{-1}), which were predicted based on soil erosion rates and pond area (Lv et al., 2024). The current depth of the pond was estimated by subtracting the sedimentation depth from the original depth. The detailed pond area and mean depth from 1960 to 2020 can be found in Table S3.

2.4.2. Nitrogen and phosphorus concentrations in ponds

Nutrient concentrations are strong predictors of CH_4 emissions (Beaulieu et al., 2019). Nitrogen (N) and phosphorus (P) levels in ponds depend on inputs from their catchments as well as biogeochemical processes within the ponds (Chen et al., 2021b; Meng et al., 2022). In this study, we assumed that nutrient concentrations were primarily driven by nutrient inputs. Additionally, we considered that ponds within the same HL-8 watershed have similar nutrient concentrations. Specifically, N and P loss by runoff from pond watersheds were used to predict average total nitrogen (TN) and total phosphorus (TP) concentrations in ponds within each HL-8 watershed.

Data on TN and TP concentrations were compiled from published literature using keywords such as "nitrogen concentration" and "phosphorus concentration." This, combined with measurements from sampled ponds, yielded a database of water quality data for 458 Chinese ponds reported in 14 studies (Table S4).

To estimate N and P runoff, we used the NUtrient flows in Food chains, Environment, and Resources use (NUFER) model (Lv et al., 2024; Wang et al., 2018) at the HL-8 watershed scale from 1960 to 2020 (Fig. S2). Inputs for N and P runoff calculations included data on fertilizer use, livestock numbers, and human population sizes, derived from Provincial Statistical Yearbooks.

Using the TN and TP concentrations (*TN_pond* and *TP_pond*, $\mu g\, l^{-1}$)for the ponds sampled during this study and the literature, we established relationships between pond water quality and the corresponding nutrient runoff (*Nrunoff_HL-8 and Prunoff_HL-8*, $kg\, ha^{-1}\, yr^{-1}$) at the HL-8 watershed scale (Table S4), yielding the following equations:

$$TN_{pond} = 43 \times Nrunoff\_HL-8 + 870\ (R^2 = 0.41,\ p < 0.001,\ n = 31) \quad (4)$$

$$TP_{pond} = 29 \times Prunoff\_HL-8 + 12\ (R^2 = 0.38,\ p < 0.01,\ n = 31) \quad (5)$$

TN and TP concentrations from 1960 to 2020were predicted by N and P runoff across China using these equations.

2.5. Uncertainty analysis

A Monte Carlo simulation was conducted to the uncertainty in estimating CH_4 emissions. The primary sources of uncertainty considered were the predictive model for CH_4 emission rates at the standardized temperature, the temperature dependence of CH_4 emissions, and the pond area. For the first two sources, Gaussian distributions were modeled using regression coefficients and their associated standard errors (Harrison et al., 2021). To address uncertainty in pond water area, we applied a 10 % standard deviation on either side for the Monte Carlo simulations, estimating variability in CH_4 flux. Our study reports median flux estimates, supplemented by 5th to 95th percentile confidence interval bounds from these simulations.

To further assess sensitivity, we applied a one-variable-at-a-time approach to evaluate how variations in input variables—pond area, temperature, water depth and TN concentrations—affect CH_4 fluxes. We examined scenarios where each target variable deviated by −20 % to +20 % from its mean value, while holding other inputs constant, to evaluate the sensitivity of CH_4 emission fluxes.

2.6. Statistical analyses

We used variation partitioning modeling to quantify the relative contributions of four groups of factors in explaining changes in total CH_4 flux from 1960 to 2020. These four groups of factors included: (1) pond water surface area, (2) temperature, (3) water depth and (4) water nutrient. The variation partitioning model was performed based on R package Vegan (Oksanen et al., 2013).

3. Results

3.1. CH_4 emission rates from ponds

Analysis of the compiled dataset (Table S2) revealed substantial variation in total CH_4 emission rates (diffusive flux and ebullition) from ponds (Table 1), with an average of 151.6 mg CH_4 m^{-2} day^{-1}. Diffusive emissions averaged 40.5 mg CH_4 m^{-2} day^{-1}, while ebullition exhibited a notably higher mean rate of 111.02 mg CH_4 m^{-2} day^{-1}. CH_4 emission rates were further categorized by eco-climatic pond types. Surprisingly, tropical/subtropical ponds exhibited the lowest emission rates, whereas temperate and boreal ponds showed higher rates. Ebullition was identified as the dominant CH_4 emission pathway, contributing an average of 80 % to total emissions (median: 88 %, 95 % confidence interval (CI): 5.6 %–99.6 %). Additionally, the contribution of ebullition to total CH_4 emissions increased with rising water temperature and decreasing water depth (Fig. 2).

3.2. Temperature dependence of pond CH_4 emissions

In our compiled dataset, CH_4 emission rates from ponds increased exponentially with water temperature ($P < 0.001$; Fig. S3a). Analyzing the two primary emission pathways, field data showed that CH_4 ebullitive emissions had an exponential relationship with water temperature ($P < 0.001$; Fig. S3c), while diffusive CH_4 emissions did not exhibit a similar dependency. To characterize the temperature dependence of pond CH_4 emissions, we fitted the Boltzmann–Arrhenius function to the data in the compilation database. The apparent activation energy (reflecting the temperature dependence) of total CH_4 (E_{TM}) emissions was 0.83 eV (95 % CI: 0.68 to 0.98) (Fig. 3a). As for two emission pathways, activation energy of CH_4 ebullitive emissions (E_{EM}, 1.43 eV, 95 % CI: 0.94 to 1.86; Fig. 3c) differed significantly from that of diffusive

Table 1
CH_4 emission rates from Ponds.

Emission rate mg CH_4 m^{-2} day^{-1}	Eco-climatic region	Mean	Median	95 % CI	n
Diffusive	/	40.50	14.24	0.6–388.77	318
Ebullitive	/	111.02	73.29	0.21–563.36	192
Total	/	151.60	76.80	2.18-1079.04	512
	Boreal	122.61	43.91	1.35–1215	214
	Temperate	188.73	155.23	4.51–942.57	138
	Tropical/ Subtropical	150	72.15	2.08–905	146

Note: Boreal (>50°N or >50°S), Temperate (23.5°N-50°N or 23.5°S-50°S), Tropical/Subtropical (23.5°S-23.5°N), 95 % CI: 95 % confidence interval (CI), n is number of observations.

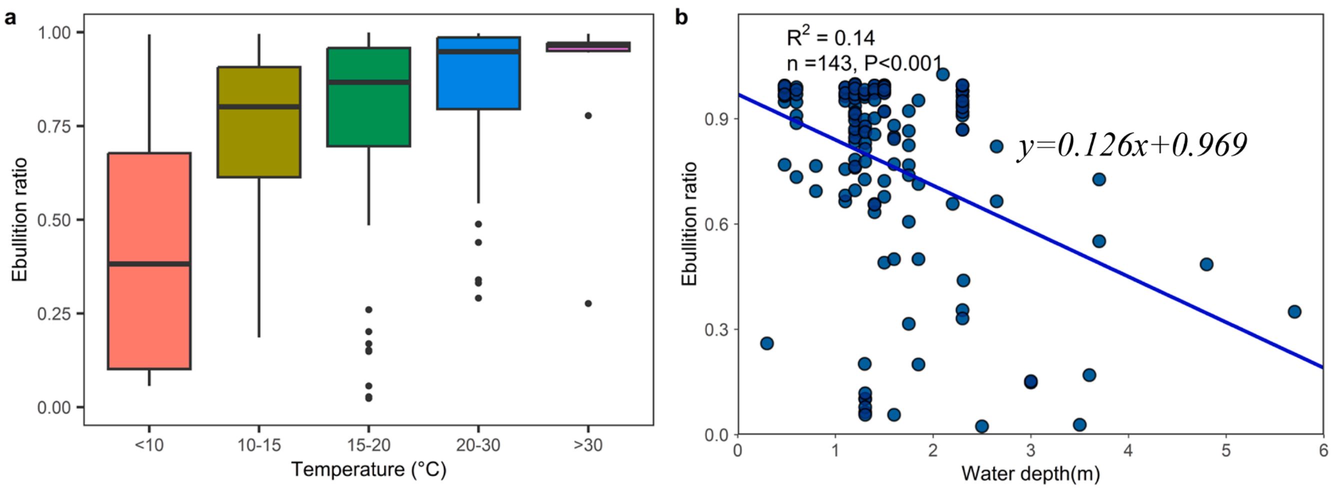

Fig. 2. Relationship between ebullition rate and water temperature (a), water depth (b). The temperature on the x-axis indicates the air temperature when measuring the CH4 emission rate. n represents the number of samples.

emissions ($E_{DM,}$ 0.54 eV, 95 % CI: 0.17 to 0.83; Fig. 3b), suggesting that ebullitive emissions showed higher temperature dependence than diffusive emissions.

As expected from the different responses of ebullitive and diffusive emissions to temperature, the proportion of ebullitive emissions to total emissions was significantly affected by temperature across all sites (Fig. 3d). This result suggests that, on average, the relative contribution of ebullition to total CH_4 emissions rises with seasonal temperature increases or in the context of climate warming.

3.3. Drivers and predicting models of CH_4 emissions

Utilizing our compiled dataset, we examined the relationship between total CH_4 emission rates at a standardized water temperature (19 °C) and various climatic, morphometric, water nutrient, and biotic variables through a linear mixed-effects model (Fig. 4). Climatic variables, including MAT and MAP, showed a significant negative correlation with total areal CH_4 emissions. Regarding morphometric features, CH_4 emissions significantly declined with increasing water column depth, although no significant relationship was observed between water surface area and CH_4 emissions. Among water nutrient variables, total nitrogen (TN), total phosphorus (TP), and ammonium (NH_4^+) significantly influenced total areal CH_4 emissions, while nitrate (NO_3^-) did not show a regulatory effect. DOC exhibited significantly relationship with total CH_4 emissions, while Chl-a had a marginally significant effect on total emissions.

Climatic variables were particularly influential on standard-temperature diffusive CH_4 emissions, while no similar relationship was observed for ebullitive CH_4 emissions. The slope of water depth on ebullitive emissions was larger than that on diffusive emissions, indicating water depth likely more strongly regulates ebullition relative to diffusive fluxes. Major nutrient variables present significantly positive relationship with diffusive emissions, but significant relationships between nutrient variables and areal ebullitive CH_4 emissions were not observed, possibly due to limited sample size. Overall, the relationship between environmental properties and two CH_4 emission pathways was weaker than their relationship with total CH_4 emissions, complicating the upscaling of individual CH_4 pathways based solely on environmental factor correlations.

The potential regression models for CH_4 total emission rates are presented in Table S5. When including TN, TP, and depth of ponds, the predicting equation can have a higher R^2 and a lower RMSE. However, two of its predictor variables are not statistically significant (TP and Depth). When using TN and depth as predictors, the equation shows only a slightly lower R^2 and a slightly higher RMSE compared to the original three-variable model, and both variables are statistically significant. Thus, the best-performing regression equation for pond CH_4 emissions at the standard-temperature for ponds used TN and depth variables, as follow:

$$\ln(R_{base}) = 0.95 \times \ln(TN_{pond}) - 0.51 \times \ln(H) - 0.23$$

where R_{base} is pond CH_4 emission rates ($mg\ m^{-2}\ day^{-1}$), is TN concentration ($\mu g\ L^{-1}$) and H is water depth (cm).

3.4. CH_4 emission flux from 1960 to 2020

The spatial distribution of annual CH_4 emission across China from 1960 to 2020 were modeled using the best-predicting model (Fig. 5a–g). During this period, annual CH_4 emission flux from ponds increased 8.6-fold, rising from 0.16 Tg CH_4 yr^{-1} (95 % CI: 0.09–0.24 Tg CH_4 yr^{-1}) in 1960 to 1.53 Tg CH_4 yr^{-1} (95 % CI: 0.85–2.22 Tg CH_4 yr^{-1}) in 2020 (Fig. 5h). On average, the annual growth rate of pond CH_4 emissions over this period was approximately 0.02 Tg CH_4 yr^{-1}. Seasonal analysis revealed that CH_4 emissions during the summer season accounted for approximately half of the total annual flux, followed by emissions during autumn (23.9 %) and spring (21.6 %), with winter contributing only 7.8 % of the total annual emissions in 2020. Notable hotspots for CH_4 emissions were identified in the eastern Yangtze River Basin and the southern Huaihe River Basin (Fig. 5). In 2020, pond ebullition fluxes were 0.99 Tg CH_4 yr^{-1}, contributing around 66 % of total CH_4 emissions, with a higher contribution observed in the tropical climates of Southern China. Very small ponds (<0.1 ha) account for 40.6 % of total CH_4 emissions, but comprise 21.54 % of ponds by area in Chinese (Table S6). However, large ponds (>2 ha) contribute only 9.15 % of CH_4 fluxes, while covering 18.87 % of pond area.

3.5. Sensitivity and contributions for CH_4 flux

In a sensitivity analysis, we evaluated the changes in pond CH_4 emission fluxes when input variables decreased or increased by 20 % (Fig. 6). CH_4 emissions were most sensitive to temperature changes. Specifically, CH_4 fluxes decreased by up to 28.6 % and increased by as much as 39.3 % when air temperature was reduced or increased by 20 % from the base level. This indicates that CH_4 emissions are more strongly influenced by climate warming than by cooling. CH_4 emission fluxes showed the same changes as pond area. Regarding water nutrient and depth, CH_4 emissions were more sensitive to TN concentration than to water depth. Overall, ±20 % changes in nitrogen concentration led to

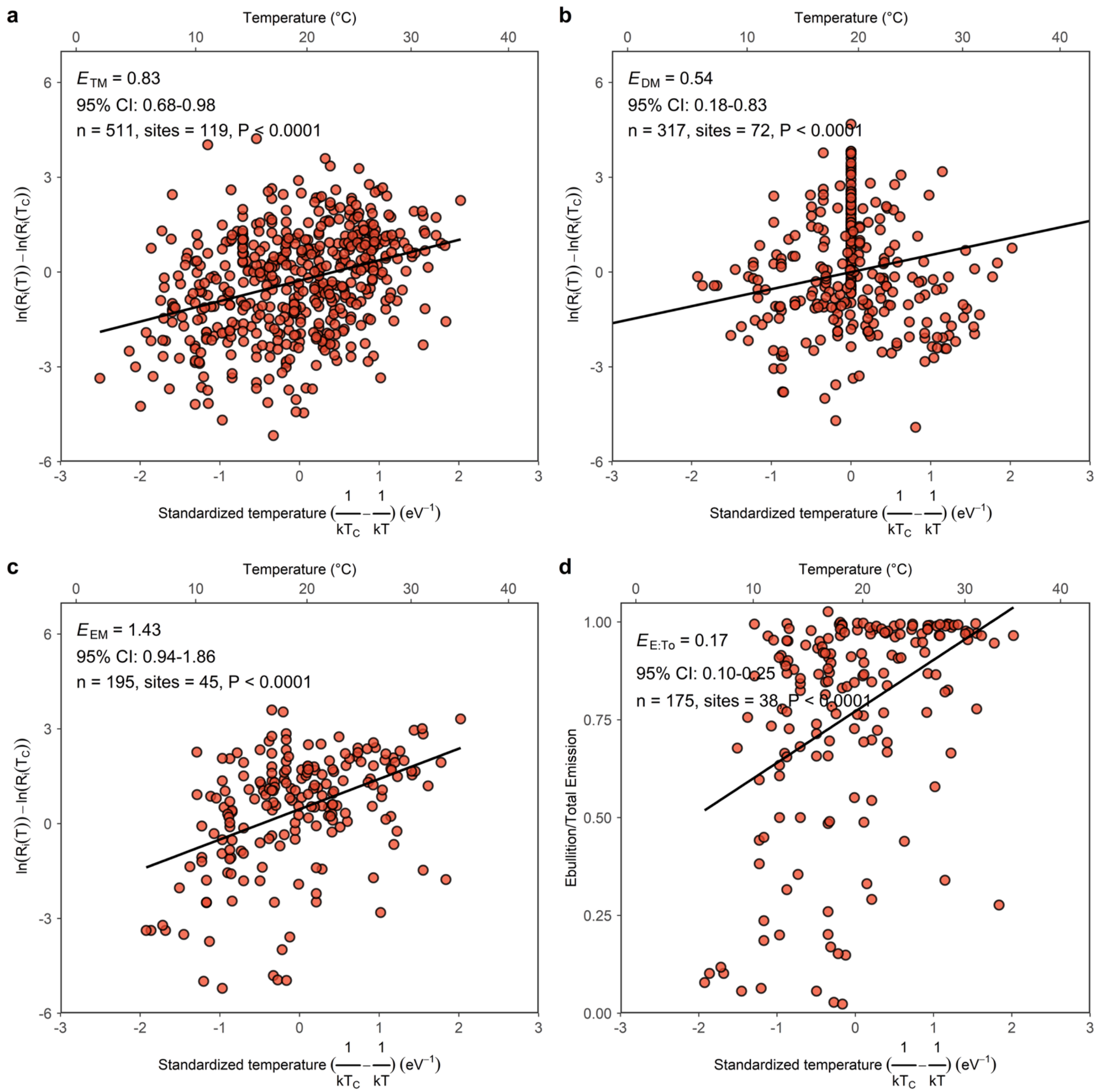

Fig. 3. Temperature dependence of pond CH_4 emissions. The temperature dependence values of pond total (a), diffusive (b), ebullitive (c) emissions and ebullitive:total emission ratio(d) were separately characterized using mixed-effects models after fitting Boltzmann–Arrhenius functions to the emissions data. The fitted solid lines correspond to the average apparent activation energies estimated from the mixed-effects models (E_{TM} = 0.83 eV for the total CH_4 emissions (**a**), E_{DM} = 0.54 eV for the diffusive CH_4 emissions (**b**), E_{EM} = 1.43 eV for the ebullitive CH_4 emissions (**c**), $E_{E:D}$ = 0.17 eV for ebullitive:total emission ratio (**d**)). **a,b,c** Emissions are expressed in standardized form as $\ln[R_i(T)]$-$\ln[R_i(T_C)]$, where $R_i(T)$ is the measured CH_4 emission rate at site i and $R_i(T_C)$ is the site-specific estimate of the CH_4 emission rate at a fixed temperature (T_C = 19 °C, the average measured temperature in the complied emissions dataset). n represents the number of samples.

CH_4 flux variations ranging from −19.5 % to +18.6 %.

When considering the single contributions of four factors, water depth accounted for the largest proportion of variance in CH_4 fluxes. However, most of the variance in CH_4 emissions was explained by interactions among factors. The combined influence of all four variables explained 29 % of the variance, while the interaction between nutrient concentration and depth accounted for 28 %. Furthermore, the interaction among nutrient concentration, depth, and pond area explained 30 % of the variance.

4. Discussion

4.1. High CH_4 emission rate and ebullition proportion from ponds

Among aquatic ecosystem, ponds exhibit particularly high CH_4 emission rates with a mean of 151.60 mg CH_4 m^{-2} day^{-1}, and a median of 76.8 mg CH_4 m^{-2} day^{-1}. These values are substantially higher than CH_4 emissions from rivers and streams, which have median diffusive and ebullitive rates of 2.51 and 2.05 mg CH_4 m^{-2} day^{-1}, respectively (Rocher-Ros et al., 2023). Comparing to a global synthesis of reservoir emissions (Johnson et al., 2021), CH_4 emission rates in

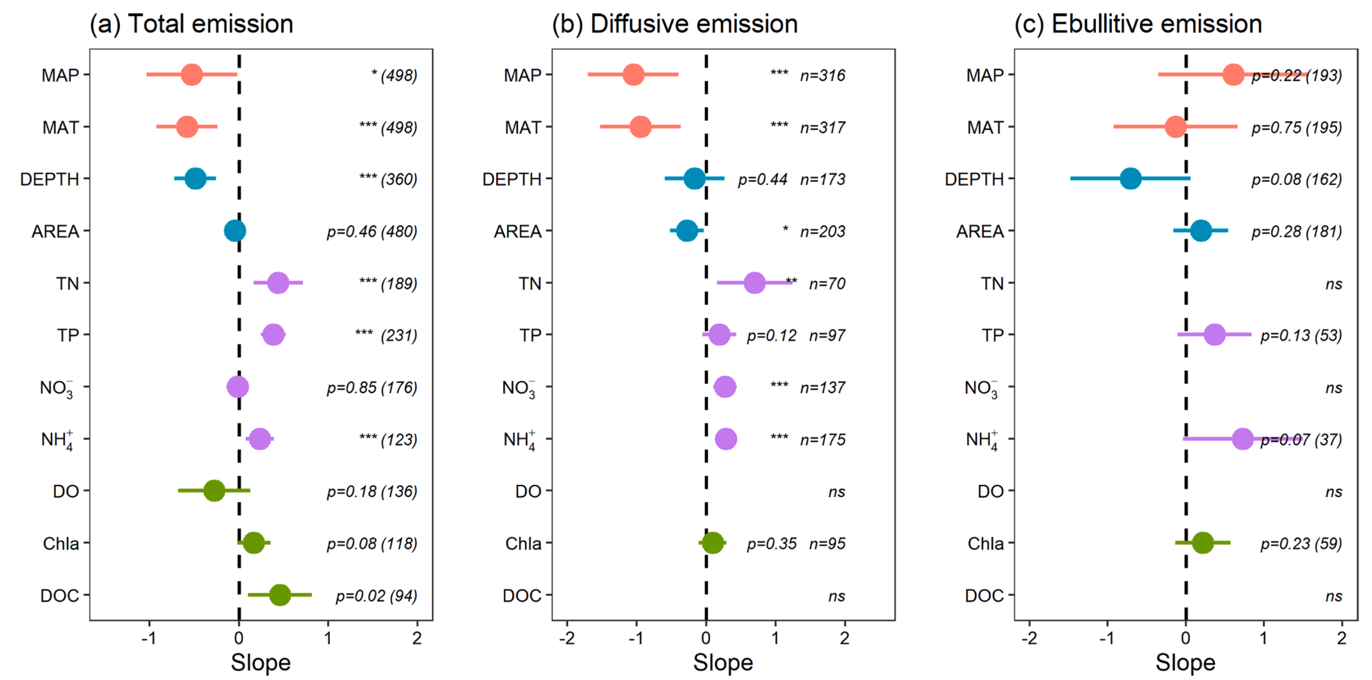

Fig. 4. Linear mixed-effects model showing relationships between CH_4 emissions and various pond variables. (a–c) Relationships between CH_4 emissions and key environmental drivers in ponds. Variables include MAP (mean annual precipitation), MAT (mean annual atmospheric temperature), DEPTH (pond water column depth), AREA (pond water surface area), TN (total nitrogen), TP (total phosphorus), NO_3^- (nitrate), NH_4^+ (ammonium), DO (dissolved oxygen), DOC (dissolved organic carbon) and Chl-a. Error bars represent 95 % confidence intervals (CIs). Effects were considered statistically significant if the 95 % CI did not overlap zero. Statistical significance is indicated by: $*p < 0.05$; $**p < 0.01$; $***p < 0.001$. Numbers in parentheses represent the number of observations in the compiled datasets.

tropical/subtropical and temperate ponds were similar to their corresponding reservoir counterparts, while boreal ponds exhibited higher emission rates than boreal reservoirs (mean 39.1 mg CH_4 m^{-2} day^{-1}). In some studies, ponds have been grouped with lakes for CH_4 emission analyses. However, when considering lakes with larger surface areas, pond emissions were higher than those from lakes of 0.1–1 km^2 (median: 20.8 mg CH_4 m^{-2} day^{-1}, $n = 58$) and lakes larger than 1 km^2 (median: 13.7 mg CH_4 m^{-2} day^{-1}, $n = 20$) (Rosentreter et al., 2021). Although the 2019 IPCC Refinement report estimated a refined CH_4 emission rate of 18.3 g m^{-2} yr^{-1} for ponds (based on a sample of 68 data points) (IPCC, 2019), our study indicates this rate may be underestimated.

Ebullition, accounting for approximately 80 % of total CH_4 emissions from ponds, is the predominant emission pathway. This proportion is comparable to that of reservoirs (median: 77.9 %) and higher than that observed in lakes (median: 53.7 %) (Deemer and Holgerson, 2021). In highly eutrophic ponds, ebullition can contribute up to 90 % of total emissions (Yang et al., 2020).

4.2. Temperature dependence

The temperature dependence of pond CH_4 emissions was greater than the larger freshwaters with the activation energy of 0.63 eV (Kraemer et al., 2017) and wetlands with 0.63 eV (0.52–0.75) (H. Chen et al., 2021a). Our estimate of activation energy is higher than the result which reported a 0.43 eV for pond CH_4 emissions based on 286 observations(Malerba et al., 2022a). This lower activation energy is likely because most of those observations included only diffusive emissions while neglecting ebullition (Ollivier et al., 2019; Webb et al., 2019).

Our findings demonstrate that ebullitive CH_4 emissions from ponds are more temperature-sensitive than diffusive emissions (Wik, 2014; DelSontro et al., 2016). Consequently, the proportion of ebullitive fluxes to total CH_4 emissions is expected to disproportionately increase with rising seasonal temperature or ongoing climate warming. The relationship between water temperature and ebullition proportion could demonstrate this point (Fig. 2a). Specifically, ebullition rate accounted for only 27 % of the total CH_4 emissions when water temperature was below 10 °C but rose to 69 % at temperatures between 10 °C and 15 °C, and further to 88 % when water temperatures exceeded 30 °C (Fig. 2a). This trend underscores that ebullition becomes the dominant CH_4 emission pathway above 10 °C, consistent with mesocosm experiments reported by Aben et al. (2017).

CH_4 fluxes are ultimately driven by methanogenesis rates (Yvon-Durocher et al., 2014a), which are enhanced by rising temperatures through increased activity of methanogenic and methanotrophic bacteria in sediments. However, while diffusive CH_4 emissions are more susceptible to oxidation by methanotrophs in the water column, ebullitive CH_4 emissions bypass this oxidation process, making them more sensitive to temperature increases (Aben et al., 2017). Previous studies have also shown that temperature has a weaker effect on CH_4 oxidation than on CH_4 production (Duc et al., 2010), reinforcing the observed temperature dependence of diffusive CH_4 emissions.

An intriguing outcome of our study is negative relationship between MAT and pond CH_4 emissions at the standardized temperature of 19 °C. This result signifies that boreal ponds had high CH_4 emission rates than tropical/subtropical ponds at the standard temperature. Indeed, this pattern is confirmed by CH_4 emission data across different eco-climatic regions in our compiled dataset (Table 1). In boreal ponds, organic substrate accumulation during the colder months fuels methanogenesis during the subsequent warming phase (Chang et al., 2021; Gedney et al., 2004), leading to higher CH_4 emissions in the warm season. This implies that boreal ponds, abundant in northern regions, may respond more intensely to climate warming, making them significant hotspots for CH_4 emissions (Wik et al., 2016).

4.3. Pond shallowing enhances CH_4 emissions

Ponds are becoming increasingly shallow due to sedimentation processes, a widespread issue that affects their ecological functions and morphometric characteristics (Ahmad et al., 2021; Renwick et al., 2005). Over the past six decades, the average depth of ponds smaller

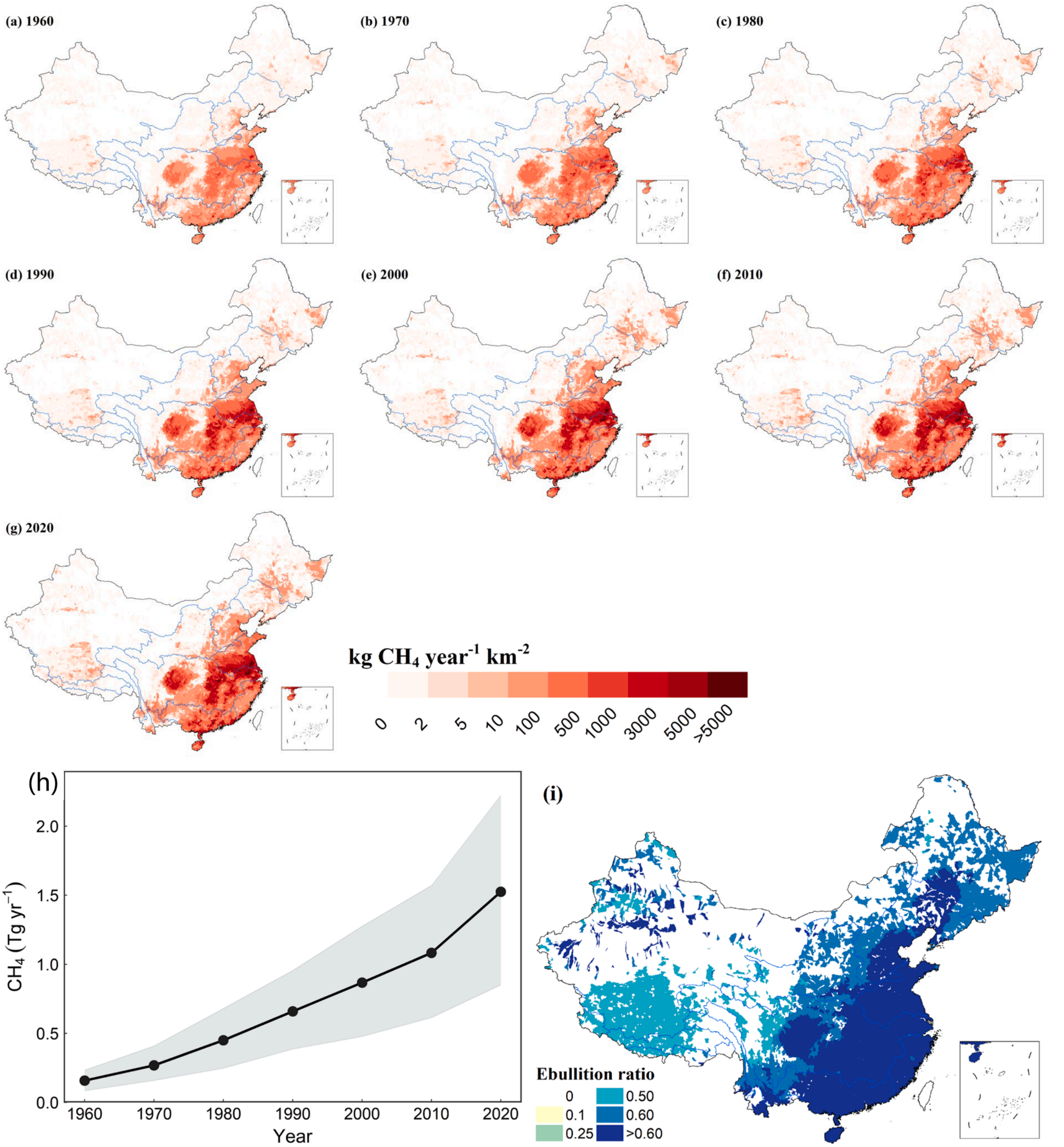

Fig. 5. Spatial and temporal changes in pond CH_4 emissions in China.
(a–g) Modeled spatial distribution of CH_4 emissions rate per HL-8 watershed area for the years 1960 (a), 1970 (b), 1980 (c), 1990 (d), 2000 (e), 2010 (f), and 2020 (g). The rates were calculated by dividing the total pond CH_4 emissions in a HL-8 watershed, in kg CH_4 per year, per the total HL-8 watershed area. (h) Temporal change in CH_4 emission fluxes from ponds in China from 1960 to 2020, with shaded areas representing the 95 % confidence intervals. (i) Spatial distribution of the ratio of ebullition to total CH_4 emissions in the HL-8 watershed in 2020, simulated using the temperature dependence of the ebullition:total CH_4 emission ratio based on the Boltzmann–Arrhenius function.

than 0.1 ha has declined sharply from 2.02 m to 0.7 m, while those between 0.1 and 1 ha have decreased from 3.21 m to 2.1 m (Table S3).

Our result confirm that water depth plays a critical role in regulating CH_4 emissions from aquatic ecosystems (Natchimuthu et al., 2016; West et al., 2016; Zhong et al., 2023). Depth not only influences the magnitude of CH_4 fluxes but also alters the dominant emission pathway. Shallow ponds exhibit a higher proportion of ebullition relative to total CH_4 emissions compared to deeper ponds. Specifically, the ebullition contribution increased by 12 % for every 1 m decrease in depth (Fig. 2b). Moreover, depth had a stronger effect on ebullitive emissions (slope=−0.7, $p = 0.08$) than on diffusive emissions (slope=−0.17, $p = 0.22$) (Fig. 4). Interestingly, this stronger impact of water column depth

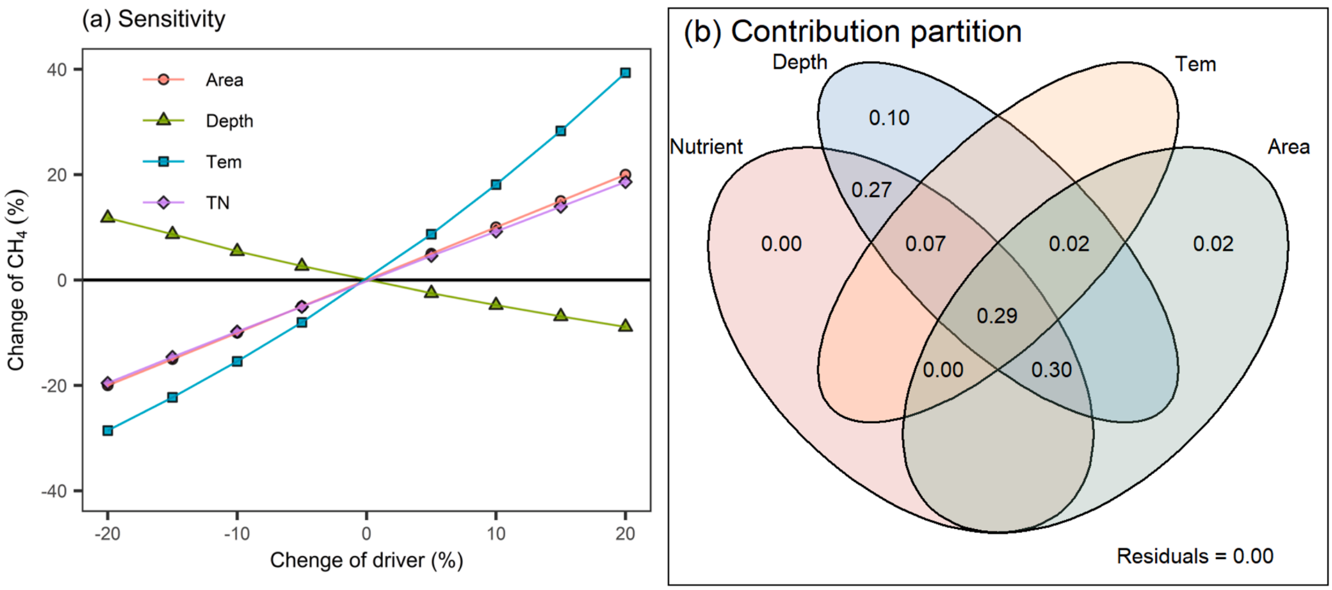

Fig. 6. Sensitivity and contribution of input drivers to CH_4 emission fluxes.
(a) Sensitivity of input drivers for CH_4 emission fluxes in 2000. (b) Relative contributions of four factors to the increase in CH_4 fluxes from 1960 to 2020, as determined by variation partitioning modeling. Factors include: TEM (mean annual air temperature), TN (total nitrogen concentration in ponds), DEPTH (pond water depth), and Area (pond area).

on pond ebullition contrasts with findings for lakes (Li et al., 2020), where lake CH_4 diffusive fluxes correlate significantly with depth, while ebullition remains relatively unaffected.

Two key mechanisms likely explain the depth-related increase in pond CH_4 ebullition. First, hydrostatic pressure, which limits bubble formation and release from sediments, is lower in shallow water bodies, thereby facilitating CH_4 ebullition (Varadharajan and Hemond, 2012; West et al., 2016). Second, water depth influences sediment temperature, a key driver of methanogenesis. Bottom sediments are the principal sites for CH_4 production in aquatic systems (Bastviken et al., 2004). Shallow sediments can be heated more effectively due to direct solar radiation or changes in epilimnion temperatures, which raises sediment temperatures (Wik et al., 2014). Elevated temperatures enhance CH_4 production by stimulating methanogenic microbes (Zhu et al., 2020). As previously noted, ebullition emission increased disproportionately with an increase in temperature. Consequently, we observed a stronger negative relationship between water depth and ebullitive CH_4 emissions than with diffusive emissions (Fig. 4). Additionally, shallow water bodies have shorter CH_4 transport pathways to the air-water interface, reducing the potential for CH_4 oxidation by methanotrophic bacteria during transport (Bastviken et al., 2010; West et al., 2016).

Overall, these findings highlight that ongoing pond shallowing due to sedimentation may significantly amplify CH_4 emissions, primarily through increased ebullition. Given the widespread occurrence of sediment accumulation in ponds globally, this process could represent an underappreciated yet increasingly important driver of CH_4 fluxes from inland waters.

4.4. Nutrient enrichment drives pond CH_4 emissions

Pond eutrophication is a widespread and pressing water environmental issue, often leading to algal blooms, oxygen depletion (Janssen et al., 2021). Chl-a, a widely used proxy of algal productivity, exhibits high concentrations in eutrophic ponds. Based on our compiled dataset (Table S2), the mean Chl-a concentration in ponds reached 56.58 μg L^{-1} (0.4 to 348.1 μg L^{-1}). Chinese ponds are usually located nearby croplands for irrigation purposes (Lv et al., 2022) and receive substantial nutrient inputs, leading to even higher Chl-a levels. For instance, in a watershed study encompassing 28 ponds, the mean Chl-a concentration was 61.7 μg L^{-1}, with values ranging from 13 to 325.28 μg L^{-1} (Xiao et al., 2023).

Although not statistically significant, Chl-a had a marginally significant effect on CH_4 emissions ($p = 0.08$), suggesting a potentially strong influence. High algal productivity enhances labile organic carbon availability, stimulating methanogenesis in sediments and thereby increasing CH_4 fluxes (Berberich et al., 2020; West et al., 2015). Furthermore, the decomposition of organic matter depletes oxygen, creating an anoxic environment that favors methanogenic bacteria (Liikanen et al., 2002), and reduce CH4 oxidation rates, and ultimately enhance diffusive CH_4 flux (Yan et al., 2017).

Eutrophication in ponds is primarily driven by external nutrient inputs from surrounding watersheds. Our analysis revealed a significant positive relationship between CH_4 emissions—particularly diffusive and total emissions—and TN and TP concentrations. However, the correlation between ebullition and nutrient levels was weaker. This could be due to the stochastic nature of ebullition, which makes it inherently difficult to measure and predict, as well as the limited number of available measurements. While TP has traditionally been considered a key predictor of CH_4 emissions in inland waters (Beaulieu et al., 2019; DelSontro et al., 2016), our findings suggest that TN may be a stronger predictor for CH_4 emissions in ponds.

Additionally, ammonium (NH_4^+) showed a significant positive correlation with both diffusive and total CH_4 emissions, and a near-significant relationship with ebullitive emissions ($p = 0.08$). This aligns with previous studies, which have also highlighted the role of NH_4^+ in driving CH_4 fluxes (Cui et al., 2024; Deng et al., 2024; Zhao et al., 2025). Methanotrophs rely on methane monooxygenase to oxidize CH_4 (Holmes et al., 1995); however, under high NH_4^+ conditions, methanotrophs preferentially utilize NH_4^+, thereby reducing CH_4 oxidation efficiency. Consequently, nitrogen-enriched aquatic environments may promote methane accumulation, ultimately leading to elevated CH_4 emissions (Bodelier and Steenbergh, 2014).

4.5. Amplifying pond CH_4 emissions in China

From 1960 to 2020, CH_4 emissions from Chinese ponds increased approximately 9-fold, underscoring their growing role in global inland water carbon fluxes. In 2020, CH_4 emissions from ponds in China reached 1.53 Tg CH_4, surpassing the estimated 0.8 Tg CH_4 from reservoirs across eastern Asia, including China (Lauerwald et al., 2023b). CH_4 emissions from rice cultivation have long been recognized as one of the dominant contributors to anthropogenic greenhouse gas emissions (Tian et al., 2016). Chinese pond, covering approximately 11.2 % of the total paddy rice cultivation area (301,400 km^2), contributed 18.6 % - 22.5 % of the CH_4 flux from rice fields in 2020, which release 6.8–8.2 Tg of CH_4 annually (Wang et al., 2021; Zhang et al., 2011). Notably, ponds smaller than 1 ha account for 81 % of total CH_4 emissions (Table S6), consistent with previous studies emphasizing the disproportionate CH_4 contribution from small ponds (DelSontro et al., 2018; Holgerson and Raymond, 2016). Interestingly, our meta-analysis did not identify water surface area as a significant driver of CH_4 emissions from ponds (Fig. 4), diverging from patterns observed in lakes and reservoirs, where surface area is a key determinant of CH_4 flux (Deemer and Holgerson, 2021).

The relative contribution of CH_4 emissions to total carbon flux is anticipated to continue rising. Since 1960, nitrogen runoff has increased tenfold (Lv et al., 2024; Yu et al., 2019), leading to widespread pond eutrophication, particularly after the 1980s. Recent studies demonstrate that nutrient enrichment drives significant increases in total CH_4 flux, along with a higher proportion of ebullitive CH_4 emissions (Davidson et al., 2018). Additionally, with increasing eutrophication, CO_2 emissions from inland waters generally decrease (Colas et al., 2021; Ran et al., 2021; Sun et al., 2021), indirectly increasing CH_4's share of total carbon emissions.

Among four key factors analyzed, CH_4 emissions exhibited the highest sensitivity to temperature (Fig. 6). As discussed earlier, temperature directly regulates CH_4 emissions by influencing methanogenesis rates (Yvon-Durocher et al., 2014a). Between 2010 and 2020, China experienced rapid temperature increases (Wang et al., 2024), coinciding with the most substantial rise in CH_4 fluxes during this period—a 0.44 Tg CH_4 increase. These findings highlight the potential for future climate warming to further amplify CH_4 emissions from Chinese ponds, emphasizing the urgent need for targeted management strategies.

4.6. Implications for pond management and limitation

Ongoing climate warming, eutrophication, and sediment accumulation are expected to further elevate CH_4 emissions from ponds. Ponds are becoming more significant contributors to global inland water carbon fluxes. As critical CH_4 emission hotspots, ponds should be explicitly accounted for in greenhouse gas inventories to improve emission estimates and mitigation strategies.

China has committed to reaching a peak in carbon emission by 2030 and then achieving carbon neutrality by 2060. Nature-based solutions, including those provided ponds, have a potentially important role to play in achieving these targets (Yang et al., 2022). Several management actions could be implemented in order to increase the potential for carbon sequestration in ponds via enhancing carbon burial and reducing CH_4 emissions.

A key management strategy is reducing nutrient input into ponds, as nutrient loading is a major driver of CH_4 emissions (Beaulieu et al., 2019). In China, high levels of nutrient runoff are primarily driven by fertilizer use (Lv et al., 2024; Xiao et al., 2024). Reducing fertilizer application could therefore maintain clearer water conditions and substantially lower CH_4 emissions from ponds. Additionally, reducing the rising N:P ratio in aquatic systems, driven by human activities (Wu et al., 2022), could mitigate CH_4 emissions in eutrophic inland waters (Yu et al., 2025). Increasing pond depth also holds promise for reducing emissions due to enhanced CH_4 oxidation in the sediment layer before it reaches the water surface (Webb et al., 2019). Given the significant sedimentation in Chinese ponds, periodic dredging of shallow ponds can maintain adequate water depth, thereby improving water quality, reducing organic substance supply and reducing CH_4 flux.

Only a minority of the studies in our database reported sediment temperatures. Improved measurements of temperatures at the sediment-water interface would greatly enhance present and future CH_4 emission estimates. Besides, due to the limited availability of simultaneous CH_4 emissions and sediment property measurements, our study couldn't directly qualify the relationship between CH_4 emissions and sediment characteristics. Quantifying monthly nutrient concentration changes across millions of ponds remains a significant challenge, but better estimates of pond productivity and nutrient levels would improve CH_4 flux assessments. Additionally, ponds are highly susceptible to anthropogenic disturbances and climate fluctuations, which cause substantial changes in surface water area and depth across wet and dry seasons. These water level fluctuations likely impact CH_4 emissions, suggesting that future assessments should incorporate these dynamic factors (Keller et al., 2021; Malerba et al., 2024). Remote sensing provides large-scale monitoring of key environmental variables and captures their spatio-temporal dynamics (Asadollah et al., 2025; Kuhn et al., 2019; Sun et al., 2024). Future research can further integrate remote sensing technology and machine learning to enhance the accuracy and spatial applicability of CH_4 emission predictions in ponds (Duan et al., 2023). Future research should focus on leveraging these technologies to develop more precise, scalable models for assessing CH_4 emissions from ponds, ultimately aiding in more effective mitigation strategies.

5. Conclusion

This study synthesizes 674 observations to provide a comprehensive analysis of CH_4 emissions from ponds, highlighting an increasingly growing role as significant contributor to global CH4 budgets. Our findings reveal that ebullitive emissions exhibit significantly higher temperature dependence than diffusive emissions, with warming disproportionately increasing ebullition fraction. Water depth, rather than water surface area, emerges as a more influential driver and predictor of CH_4 emissions, highlighting the importance of pond shallowing as a key mechanism that not only amplifies total emissions but also shifts the dominant pathway toward ebullition. Additionally, nitrogen concentrations proved to be a more reliable predictor of CH_4 fluxes than phosphorus, underscoring the role of nutrient dynamics in regulating emissions.

We developed a spatially explicit framework to estimate CH_4 emissions from ponds, revealing that while pond area in China has doubled from 1960 to 2020, CH_4 emissions have increased approximately 9-fold, reaching 1.54 Tg CH_4 yr^{-1} in 2020. This findings suggest that ponds are intensifying as CH_4 sources and should be explicitly incorporated into national greenhouse gas inventories to emission assessments and inform mitigation strategies. Small ponds disproportionately contribute to CH_4 emissions due to their high susceptibility to sedimentation and eutrophication. Targeted interventions, such as sediment dredging and nutrient control, could serve as effective mitigation strategies. Overall, by identifying key drivers and refining previous estimates, this study provides critical insights into the growing impact of ponds on global CH_4 budgets and informs sustainable management practices.

CRediT authorship contribution statement

Mingquan Lv: Writing – original draft, Resources, Project administration, Formal analysis, Conceptualization. **Ping Huang:** Methodology, Conceptualization. **Xin Gao:** Software, Methodology, Investigation. **Jilong Chen:** Methodology, Formal analysis, Conceptualization. **Shengjun Wu:** Supervision, Resources, Conceptualization.

Declaration of competing interest

We hereby confirm that we have carefully reviewed and comprehended the Conflict of Interest Policy outlined by Water Research. We declare that we have no conflict of interest.

Acknowledgements

This research was funded by *National Key Research and Development Program of China* (Grant No 2024YFD1700200) and *National Natural Science Foundation of China* (Grant No 42071242).

Data Availability Statement

The data that support the findings of this study are available in the Supporting Information of this article.

Supplementary materials

Supplementary material associated with this article can be found, in the online version, at doi:10.1016/j.watres.2025.123576.

Data availability

Data will be made available on request.

References

Aben, R.C.H., Barros, N., van Donk, E., Frenken, T., Hilt, S., Kazanjian, G., Lamers, L.P. M., Peeters, E.T.H.M., Roelofs, J.G.M., de Senerpont Domis, L.N., Stephan, S., Velthuis, M., Van de Waal, D.B., Wik, M., Thornton, B.F., Wilkinson, J., DelSontro, T., Kosten, S., 2017. Cross continental increase in methane ebullition under climate change. Nat. Commun. 8 (1), 1682.

Ahmad, M.-u.-D., Peña-Arancibia, J.L., Yu, Y., Stewart, J.P., Podger, G.M., Kirby, J.M., 2021. Climate change and reservoir sedimentation implications for irrigated agriculture in the Indus Basin Irrigation System in Pakistan. J. Hydrol. 603, 126967.

Asadollah, S.B.H.S., Safaeinia, A., Jarahizadeh, S., Alcalá, F.J., Sharafati, A., Jodar-Abellan, A., 2025. Dissolved organic carbon estimation in lakes: improving machine learning with data augmentation on fusion of multi-sensor remote sensing observations. Water Res., 123350

Bai, Z., 1999. A new formula for calculating water temperature of lake or reservoir (in Chinese). Hydrology (3), 29–32.

Bastviken, D., Cole, J., Pace, M., Tranvik, L., 2004. Methane emissions from lakes: dependence of lake characteristics, two regional assessments, and a global estimate. Glob. Biogeochem. Cycles 18 (4), GB4009.

Bastviken, D., Santoro, A.L., Marotta, H., Pinho, L.Q., Calheiros, D.F., Crill, P., Enrich-Prast, A., 2010. Methane emissions from Pantanal, South America, during the low water season: toward more comprehensive sampling. Environ. Sci. Technol. 44 (14), 5450–5455.

Bastviken, D., Tranvik, L.J., Downing, J.A., Crill, P.M., Enrich-Prast, A., 2011. Freshwater methane emissions offset the continental carbon sink. Science (1979) 331 (6013), 50.

Beaulieu, J.J., DelSontro, T., Downing, J.A., 2019. Eutrophication will increase methane emissions from lakes and impoundments during the 21st century. Nat. Commun. 10 (1), 1375.

Berberich, M.E., Beaulieu, J.J., Hamilton, T.L., Waldo, S., Buffam, I., 2020. Spatial variability of sediment methane production and methanogen communities within a eutrophic reservoir: importance of organic matter source and quantity. Limnol. Oceanogr. 65 (6), 1336–1358.

Bodelier, P.L.E., Steenbergh, A.K., 2014. Interactions between methane and the nitrogen cycle in light of climate change. Curr. Opin. Environ. Sustain. 9-10, 26–36.

Chang, K., Riley, W., Knox, S., Jackson, R., McNicol, G., Poulter, B., Aurela, M., Baldocchi, D., Bansal, S., Bohrer, G., 2021. Substantial hysteresis in emergent temperature sensitivity of global wetland CH4 emissions. Nat Commun 12, 2266.

Chen, H., Xu, X., Fang, C., Li, B., Nie, M., 2021a. Differences in the temperature dependence of wetland CO2 and CH4 emissions vary with water table depth. Nat. Clim. Chang. 11 (9), 766–771.

Chen, W., Nover, D., Xia, Y., Zhang, G., Yen, H., He, B., 2021b. Assessment of extrinsic and intrinsic influences on water quality variation in subtropical agricultural multipond systems. Environ. Pollut. 276, 116689.

Colas, F., Baudoin, J.-M., Bonin, P., Cabrol, L., Daufresne, M., Lassus, R., Cucherousset, J., 2021. Ecosystem maturity modulates greenhouse gases fluxes from artificial lakes. Sci. Total Environ. 760, 144046.

Cui, P., Cui, L., Zheng, Y., Su, F., 2024. Land use and urbanization indirectly control riverine CH4 and CO2 emissions by altering nutrient input. Water Res. 265, 122266.

Davidson, T.A., Audet, J., Jeppesen, E., Landkildehus, F., Lauridsen, T.L., Søndergaard, M., Syväranta, J., 2018. Synergy between nutrients and warming enhances methane ebullition from experimental lakes. Nat. Clim. Chang. 8 (2), 156–160.

Deemer, B.R., Harrison, J.A., Li, S., Beaulieu, J.J., DelSontro, T., Barros, N., Bezerra-Neto, J.F., Powers, S.M., Dos Santos, M.A., Vonk, J.A., 2016. Greenhouse gas emissions from reservoir water surfaces: a new global synthesis. Bioscience 66 (11), 949–964.

Deemer, B.R., Holgerson, M.A., 2021. Drivers of methane flux differ between lakes and reservoirs, complicating global upscaling efforts. J. Geophys. Res.: Biogeosci. 126 (4) e2019JG005600.

DelSontro, T., Beaulieu, J.J., Downing, J.A., 2018. Greenhouse gas emissions from lakes and impoundments: upscaling in the face of global change. Limnol. Oceanogr. Lett. 3 (3), 64–75.

DelSontro, T., Boutet, L., St-Pierre, A., del Giorgio, P.A., Prairie, Y.T., 2016. Methane ebullition and diffusion from northern ponds and lakes regulated by the interaction between temperature and system productivity. Limnol. Oceanogr. 61 (S1), S62–S77.

Deng, M., Yeerken, S., Wang, Y., Li, L., Li, Z., Oon, Y.-S., Oon, Y.-L., Xue, Y., He, X., Zhao, X., Song, K., 2024. Greenhouse gases emissions from aquaculture ponds: different emission patterns and key microbial processes affected by increased nitrogen loading. Sci. Total Environ. 926, 172108.

Downing, J.A., Cole, J.J., Middelburg, J.J., Striegl, R.G., Duarte, C.M., Kortelainen, P., Prairie, Y.T., Laube, K.A., 2008. Sediment organic carbon burial in agriculturally eutrophic impoundments over the last century. Glob. Biogeochem. Cycles 22 (1).

Duan, H., Xiao, Q., Qi, T., Hu, C., Zhang, M., Shen, M., Hu, Z., Wang, W., Xiao, W., Qiu, Y., Luo, J., Lee, X., 2023. Quantification of diffusive methane emissions from a large eutrophic lake with satellite imagery. Environ. Sci. Technol. 57 (36), 13520–13529.

Duc, N.T., Crill, P., Bastviken, D., 2010. Implications of temperature and sediment characteristics on methane formation and oxidation in lake sediments. Biogeochemistry 100 (1), 185–196.

Gedney, N., Cox, P., Huntingford, C., 2004. Climate feedback from wetland methane emissions. Geophys. Res. Lett. 31 (20).

Goyal, V.C., Singh, O., Singh, R., Chhoden, K., Kumar, J., Yadav, S., Singh, N., Shrivastava, N.G., Carvalho, L., 2021. Ecological health and water quality of village ponds in the subtropics limiting their use for water supply and groundwater recharge. J. Environ. Manage. 277, 111450.

Gu, B., Ju, X., Chang, J., Ge, Y., Vitousek, P.M., 2015. Integrated reactive nitrogen budgets and future trends in China. Proc. Natl. Acad. Sci. 112 (28), 8792–8797.

Harrison, J.A., Prairie, Y.T., Mercier-Blais, S., Soued, C., 2021. Year-2020 global distribution and pathways of reservoir methane and carbon dioxide emissions according to the greenhouse gas from reservoirs (G-res) model. Global Biogeochem. Cycles 35 (6) e2020GB006888.

Holgerson, M.A., Raymond, P.A., 2016. Large contribution to inland water CO2 and CH4 emissions from very small ponds. Nat. Geosci. 9 (3), 222–226.

Holmes, A.J., Costello, A., Lidstrom, M.E., Murrell, J.C., 1995. Evidence that participate methane monooxygenase and ammonia monooxygenase may be evolutionarily related. FEMS Microbiol. Lett. 132 (3), 203–208.

IPCC, 2019. 2019 Refinement to the 2006 IPCC Guidelines for National Greenhouse Gas Inventories. Agriculture, Forestry and Other Land Use, Chapter 7, Volume 4. IPCC, Wetlands. Retrieved from. https://www.ipcc-ggip.iges.or.jp/public/2019rf/pdf/4_Volume4/19R_V4_Ch07_Wetlands.

Janssen, A.B., Droppers, B., Kong, X., Teurlincx, S., Tong, Y., Kroeze, C., 2021. Characterizing 19 thousand Chinese lakes, ponds and reservoirs by morphometric, climate and sediment characteristics. Water Res. 202, 117427.

Johnson, M.S., Matthews, E., Bastviken, D., Deemer, B., Du, J., Genovese, V., 2021. Spatiotemporal methane emission from global reservoirs. J. Geophys. Res.: Biogeosci. 126 (8) e2021JG006305.

Keller, P.S., Marcé, R., Obrador, B., Koschorreck, M., 2021. Global carbon budget of reservoirs is overturned by the quantification of drawdown areas. Nat. Geosci. 14 (6), 402–408.

Kirschke, S., Bousquet, P., Ciais, P., Saunois, M., Canadell, J.G., Dlugokencky, E.J., Bergamaschi, P., Bergmann, D., Blake, D.R., Bruhwiler, L., Cameron-Smith, P., Castaldi, S., Chevallier, F., Feng, L., Fraser, A., Heimann, M., Hodson, E.L., Houweling, S., Josse, B., Fraser, P.J., Krummel, P.B., Lamarque, J.-F., Langenfelds, R. L., Le Quéré, C., Naik, V., O'Doherty, S., Palmer, P.I., Pison, I., Plummer, D., Poulter, B., Prinn, R.G., Rigby, M., Ringeval, B., Santini, M., Schmidt, M., Shindell, D. T., Simpson, I.J., Spahni, R., Steele, L.P., Strode, S.A., Sudo, K., Szopa, S., van der Werf, G.R., Voulgarakis, A., van Weele, M., Weiss, R.F., Williams, J.E., Zeng, G., 2013. Three decades of global methane sources and sinks. Nat. Geosci. 6 (10), 813–823.

Kraemer, B.M., Chandra, S., Dell, A.I., Dix, M., Kuusisto, E., Livingstone, D.M., Schladow, S.G., Silow, E., Sitoki, L.M., Tamatamah, R., McIntyre, P.B., 2017. Global patterns in lake ecosystem responses to warming based on the temperature dependence of metabolism. Glob. Chang. Biol. 23 (5), 1881–1890.

Kuhn, C., de Matos Valerio, A., Ward, N., Loken, L., Sawakuchi, H.O., Kampel, M., Richey, J., Stadler, P., Crawford, J., Striegl, R., Vermote, E., Pahlevan, N., Butman, D., 2019. Performance of Landsat-8 and Sentinel-2 surface reflectance products for river remote sensing retrievals of chlorophyll-a and turbidity. Remote Sens. Environ. 224, 104–118.

Lauerwald, R., Allen, G.H., Deemer, B.R., Liu, S., Maavara, T., Raymond, P., Alcott, L., Bastviken, D., Hastie, A., Holgerson, M.A., Johnson, M.S., Lehner, B., Lin, P., Marzadri, A., Ran, L., Tian, H., Yang, X., Yao, Y., Regnier, P., 2023a. Inland water greenhouse gas budgets for RECCAP2: 1. State-of-the-art of global scale assessments. Global Biogeochem. Cycles 37 (5) e2022GB007657.

Lauerwald, R., Allen, G.H., Deemer, B.R., Liu, S., Maavara, T., Raymond, P., Alcott, L., Bastviken, D., Hastie, A., Holgerson, M.A., Johnson, M.S., Lehner, B., Lin, P., Marzadri, A., Ran, L., Tian, H., Yang, X., Yao, Y., Regnier, P., 2023b. Inland water greenhouse gas budgets for RECCAP2: 2. Regionalization and homogenization of estimates. Global Biogeochem. Cycles 37 (5) e2022GB007658.

Li, M., Peng, C., Zhu, Q., Zhou, X., Yang, G., Song, X., Zhang, K., 2020. The significant contribution of lake depth in regulating global lake diffusive methane emissions. Water Res. 172, 115465.

Liikanen, A., Murtoniemi, T., Tanskanen, H., Väisänen, T., Martikainen, P.J., 2002. Effects of temperature and oxygenavailability on greenhouse gas and nutrient dynamics in sediment of a eutrophic mid-boreal lake. Biogeochemistry 59 (3), 269–286.

Lv, M., Chen, J., Ma, M., Huang, P., Wu, S., 2024. Diminished storage capacity of ponds caused by sedimentation weakens their nitrogen removal efficiency. Water Res. 261, 121987.

Lv, M., Wu, S., Ma, M., Huang, P., Wen, Z., Chen, J., 2022. Small water bodies in China: spatial distribution and influencing factors. Sci. China Earth Sci. 65 (8), 1431–1448.

Maeck, A., DelSontro, T., McGinnis, D.F., Fischer, H., Flury, S., Schmidt, M., Fietzek, P., Lorke, A., 2013. Sediment trapping by dams creates methane emission hot spots. Environ. Sci. Technol. 47 (15), 8130–8137.

Malerba, M.E., de Kluyver, T., Wright, N., Omosalewa, O., Macreadie, P.I., 2024. Including methane emissions from agricultural ponds in national greenhouse gas inventories. Environ. Sci. Technol. 58 (19), 8349–8359.

Malerba, M.E., de Kluyver, T., Wright, N., Schuster, L., Macreadie, P.I., 2022a. Methane emissions from agricultural ponds are underestimated in national greenhouse gas inventories. Commun. Earth Environ. 3 (1), 306.

Malerba, M.E., Lindenmayer, D.B., Scheele, B.C., Waryszak, P., Yilmaz, I.N., Schuster, L., Macreadie, P.I., 2022b. Fencing farm dams to exclude livestock halves methane emissions and improves water quality. Glob. Change Biol. 28 (15), 4701.

Meng, C., Liu, H., Li, Y., Shen, J., Li, X., Wu, J., 2022. Effects of environmental and agronomic factors on pond water quality within an intensive agricultural landscape in subtropical southern China. Agric Water Manag 274, 107953.

Naslund, L.C., Mehring, A.S., Rosemond, A.D., Wenger, S.J., 2024. Toward more accurate estimates of carbon emissions from small reservoirs. Limnol. Oceanogr. 69 (6), 1350–1364.

Natchimuthu, S., Panneer Selvam, B., Bastviken, D., 2014. Influence of weather variables on methane and carbon dioxide flux from a shallow pond. Biogeochemistry 119, 403–413.

Natchimuthu, S., Sundgren, I., Gålfalk, M., Klemedtsson, L., Crill, P., Danielsson, Å., Bastviken, D., 2016. Spatio-temporal variability of lake CH4 fluxes and its influence on annual whole lake emission estimates. Limnol. Oceanogr. 61 (S1), S13–S26.

Oksanen, J., Blanchet, F.G., Kindt, R., Legendre, P., Minchin, P.R., O'hara, R., Simpson, G.L., Solymos, P., Stevens, M.H.H. and Wagner, H. 2013. Package 'vegan'. Community ecology package, version 2(9), 1–295.

Ollivier, Q.R., Maher, D.T., Pitfield, C., Macreadie, P.I., 2019. Punching above their weight: large release of greenhouse gases from small agricultural dams. Glob. Change Biol 25 (2), 721.

Peacock, M., Audet, J., Jordan, S., Smeds, J., Wallin, M.B., 2019. Greenhouse gas emissions from urban ponds are driven by nutrient status and hydrology. Ecosphere 10 (3), e02643.

Peng, S., 2019. 1-km Monthly Mean Temperature Dataset for China (1901–2022). National Tibetan Plateau Data Center, Beijing, China.

Perkins, D.M., Yvon-Durocher, G., Demars, B.O.L., Reiss, J., Pichler, D.E., Friberg, N., Trimmer, M., Woodward, G., 2012. Consistent temperature dependence of respiration across ecosystems contrasting in thermal history. Glob. Chang. Biol. 18 (4), 1300–1311.

Ran, L., Butman, D.E., Battin, T.J., Yang, X., Tian, M., Duvert, C., Hartmann, J., Geeraert, N., Liu, S., 2021. Substantial decrease in CO2 emissions from Chinese inland waters due to global change. Nat. Commun. 12 (1), 1730.

Ray, N.E., Holgerson, M.A., Andersen, M.R., Bikše, J., Bortolotti, L.E., Futter, M., Kokorīte, I., Law, A., McDonald, C., Mesman, J.P., Peacock, M., Richardson, D.C., Arsenault, J., Bansal, S., Cawley, K., Kuhn, M., Shahabinia, A.R., Smufer, F., 2023. Spatial and temporal variability in summertime dissolved carbon dioxide and methane in temperate ponds and shallow lakes. Limnol. Oceanogr. 68 (7), 1530–1545.

Raymond, P.A., Hartmann, J., Lauerwald, R., Sobek, S., McDonald, C., Hoover, M., Butman, D., Striegl, R., Mayorga, E., Humborg, C., 2013. Global carbon dioxide emissions from inland waters. Nature 503 (7476), 355–359.

Renwick, W.H., Smith, S., Bartley, J., Buddemeier, R., 2005. The role of impoundments in the sediment budget of the conterminous United States. Geomorphology 71 (1–2), 99–111.

Richardson, D.C., Holgerson, M.A., Farragher, M.J., Hoffman, K.K., King, K.B., Alfonso, M.B., Andersen, M.R., Cheruveil, K.S., Coleman, K.A., Farruggia, M.J., 2022. A functional definition to distinguish ponds from lakes and wetlands. Sci. Rep. 12 (1), 10472.

Rocher-Ros, G., Stanley, E.H., Loken, L.C., Casson, N.J., Raymond, P.A., Liu, S., Amatulli, G., Sponseller, R.A., 2023. Global methane emissions from rivers and streams. Nature 621 (7979), 530–535.

Rosentreter, J.A., Borges, A.V., Deemer, B.R., Holgerson, M.A., Liu, S., Song, C., Melack, J., Raymond, P.A., Duarte, C.M., Allen, G.H., Olefeldt, D., Poulter, B., Battin, T.I., Eyre, B.D., 2021. Half of global methane emissions come from highly variable aquatic ecosystem sources. Nat. Geosci. 14 (4), 225–230.

Saunois, M., Stavert, A.R., Poulter, B., 2020. The Global methane Budget 2000–2017. Earth Syst. Sci. Data 12 (3), 1561–1623.

Sobek, S., DelSontro, T., Wongfun, N., Wehrli, B., 2012. Extreme organic carbon burial fuels intense methane bubbling in a temperate reservoir. Geophys. Res. Lett. 39 (1).

Song, C., Fan, C., Zhu, J., Wang, J., Sheng, Y., Liu, K., Chen, T., Zhan, P., Luo, S., Yuan, C., 2022. A comprehensive geospatial database of nearly 100 000 reservoirs in China. Earth Syst. Sci. Data 14 (9), 4017–4034.

Sun, H., Lu, X., Yu, R., Yang, J., Liu, X., Cao, Z., Zhang, Z., Li, M., Geng, Y., 2021. Eutrophication decreased CO2 but increased CH4 emissions from lake: a case study of a shallow Lake Ulansuhai. Water Res. 201, 117363.

Sun, Y., Wang, D., Li, L., Ning, R., Yu, S., Gao, N., 2024. Application of remote sensing technology in water quality monitoring: from traditional approaches to artificial intelligence. Water Res. 267, 122546.

Tao, S., Fang, J., Ma, S., Cai, Q., Xiong, X., Tian, D., Zhao, X., Fang, L., Zhang, H., Zhu, J., 2020. Changes in China's lakes: climate and human impacts. Natl. Sci. Rev. 7 (1), 132–140.

Tian, H., Lu, C., Ciais, P., Michalak, A.M., Canadell, J.G., Saikawa, E., Huntzinger, D.N., Gurney, K.R., Sitch, S., Zhang, B., Yang, J., Bousquet, P., Bruhwiler, L., Chen, G., Dlugokencky, E., Friedlingstein, P., Melillo, J., Pan, S., Poulter, B., Prinn, R., Saunois, M., Schwalm, C.R., Wofsy, S.C., 2016. The terrestrial biosphere as a net source of greenhouse gases to the atmosphere. Nature 531 (7593), 225–228.

Toffolon, M., Piccolroaz, S., Majone, B., Soja, A.-M., Peeters, F., Schmid, M., Wüest, A., 2014. Prediction of surface temperature in lakes with different morphology using air temperature. Limnol. Oceanogr. 59 (6), 2185–2202.

van Bergen, T.J.H.M., Barros, N., Mendonça, R., Aben, R.C.H., Althuizen, I.H.J., Huszar, V., Lamers, L.P.M., Lürling, M., Roland, F., Kosten, S., 2019. Seasonal and diel variation in greenhouse gas emissions from an urban pond and its major drivers. Limnol. Oceanogr. 64 (5), 2129–2139.

Varadharajan, C., Hemond, H.F., 2012. Time-series analysis of high-resolution ebullition fluxes from a stratified, freshwater lake. J. Geophys. Res.: Biogeosci. 117 (G2).

Wang, K., Zheng, Z., Zhu, X., Dong, W., Tett, S.F.B., Dong, B., Zhang, W., Lott, F.C., Bu, L., Wang, Y., Li, H., Nanding, N., Freychet, N., Wang, D., Qiao, S., 2024. Anthropogenic influences on the extremely dry and hot summer of 2020 in Southern China and projected changes in the likelihood of the event. Weather Clim. Extrem. 45, 100706.

Wang, M., Ma, L., Strokal, M., Ma, W., Liu, X., Kroeze, C., 2018. Hotspots for nitrogen and phosphorus losses from food production in China: a county-scale analysis. Environ. Sci. Technol. 52 (10), 5782–5791.

Wang, Z., Zhang, X., Liu, L., Wang, S., Zhao, L., Wu, X., Zhang, W., Huang, X., 2021. Estimates of methane emissions from Chinese rice fields using the DNDC model. Agric. For. Meteorol. 303, 108368.

Webb, J.R., Leavitt, P.R., Simpson, G.L., Baulch, H.M., Haig, H.A., Hodder, K.R., Finlay, K., 2019. Regulation of carbon dioxide and methane in small agricultural reservoirs: optimizing potential for greenhouse gas uptake. Biogeosciences 16 (21), 4211–4227.

West, W.E., Creamer, K.P., Jones, S.E., 2016. Productivity and depth regulate lake contributions to atmospheric methane. Limnol. Oceanogr. 61 (S1), S51–S61.

West, W.E., McCarthy, S.M., Jones, S.E., 2015. Phytoplankton lipid content influences freshwater lake methanogenesis. Freshw. Biol. 60 (11), 2261–2269.

Wik, M., Thornton, B.F., Bastviken, D., MacIntyre, S., Varner, R.K., Crill, P.M., 2014. Energy input is primary controller of methane bubbling in subarctic lakes. Geophys. Res. Lett. 41 (2), 555–560.

Wik, M., Varner, R.K., Anthony, K.W., MacIntyre, S., Bastviken, D., 2016. Climate-sensitive northern lakes and ponds are critical components of methane release. Nat. Geosci. 9 (2), 99–105.

Wu, Z., Li, J., Sun, Y., Peñuelas, J., Huang, J., Sardans, J., Jiang, Q., Finlay, J.C., Britten, G.L., Follows, M.J., Gao, W., Qin, B., Ni, J., Huo, S., Liu, Y., 2022. Imbalance of global nutrient cycles exacerbated by the greater retention of phosphorus over nitrogen in lakes. Nat. Geosci. 15 (6), 464–468.

Xiao, H., Jiang, M., Su, R., Luo, Y., Jiang, Y., Hu, R., 2024. Fertilization intensities at the buffer zones of ponds regulate nitrogen and phosphorus pollution in an agricultural watershed. Water Res. 250, 121033.

Xiao, H., Luo, Y., Jiang, M., Su, R., Li, J., Xiang, R., Hu, R., 2023. Landscape patterns are the main regulator of pond water chlorophyll α concentrations in subtropical agricultural catchments of China. J. Clean. Prod. 425, 139013.

Yan, X., Xu, X., Wang, M., Wang, G., Wu, S., Li, Z., Sun, H., Shi, A., Yang, Y., 2017. Climate warming and cyanobacteria blooms: looks at their relationships from a new perspective. Water Res. 125, 449–457.

Yang, H., Huang, X., Hu, J., Thompson, J.R., Flower, R.J., 2022. Achievements, challenges and global implications of China's carbon neutral pledge. Front. Environ. Sci. Eng. 16 (8), 111.

Yang, P., Zhang, Y., Yang, H., Guo, Q., Lai, D.Y.F., Zhao, G., Li, L., Tong, C., 2020. Ebullition was a major pathway of methane emissions from the aquaculture ponds in southeast China. Water Res. 184, 116176.

Yu, C., Huang, X., Chen, H., Godfray, H.C.J., Wright, J.S., Hall, J.W., Gong, P., Ni, S., Qiao, S., Huang, G., 2019. Managing nitrogen to restore water quality in China. Nature 567 (7749), 516–520.

Yu, W., Liu, F., Jiao, X., Fan, P., Yang, H., Zhang, Y., Li, J., Chen, J., Li, X., 2025. Human-induced N-P imbalances will aggravate GHG emissions from lakes and reservoirs under persisting eutrophication. Water Res. 276, 123240.

Yvon-Durocher, G., Allen, A.P., Bastviken, D., Conrad, R., Gudasz, C., St-Pierre, A., Thanh-Duc, N., del Giorgio, P.A., 2014a. Methane fluxes show consistent temperature dependence across microbial to ecosystem scales. Nature 507 (7493), 488.

Yvon-Durocher, G., Allen, A.P., Bastviken, D., Conrad, R., Gudasz, C., St-Pierre, A., Thanh-Duc, N., del Giorgio, P.A., 2014b. Methane fluxes show consistent temperature dependence across microbial to ecosystem scales. Nature 507 (7493), 488–491.

Zhang, W., Yu, Y., Huang, Y., Li, T., Wang, P., 2011. Modeling methane emissions from irrigated rice cultivation in China from 1960 to 2050. Glob. Chang. Biol. 17 (12), 3511–3523.

Zhao, J., Zhang, M., Pu, Y., Jia, L., Xiao, W., Zhang, Z., Ge, P., Shi, J., Xiao, Q., Lee, X., 2025. Dynamic and high methane emission flux in pond and lake aquaculture. J. Hydrol. 653, 132765.

Zhong, J., Yang, F., Zhang, M., Sun, C., Wang, S., Chen, Q., Wang, H., Zhang, L., 2023. Water depth and productivity regulate methane (CH4) emissions from temperate cascade reservoirs in northern China. J. Hydrol. 626, 130170.

Zhu, Y., Purdy, K.J., Eyice, Ö., Shen, L., Harpenslager, S.F., Yvon-Durocher, G., Dumbrell, A.J., Trimmer, M., 2020. Disproportionate increase in freshwater methane emissions induced by experimental warming. Nat. Clim. Chang. 10 (7), 685–690.